A Hermitian Box-Scheme for 1D elliptic equations - Application to problems with high contrasts in the ellipticity. *

J-P. Croisille, Metz

October 2, 2006

Abstract

We introduce a new box-scheme, called "hermitian box-scheme" on the model of the one-dimensional Poisson problem. The scheme combines features of the box-scheme of Keller, [20], [13] with the hermitian approximation of the gradient on a compact stencil, which is characteristic of compact schemes, [9, 21]. The resulting scheme is proved to be 4th order accurate for the primitive unknown u and its gradient p. The proved convergence rate is 1.5 for (u, p) in the discrete L^2 norm. The connection with a non standard mixed finite element method is given. Finally, numerical results are displayed on pertinent 1D elliptic problems with high contrasts in the ellipticity, showing in practice convergence rates ranging from 1 to 2.5 in the discrete H^1 norm.

MSC Subject Classification: 35J25 - 65M15 - 65N30 - 76M12 - 76M20
Key words: Box-scheme, finite volume method, porous media equation, Keller box-scheme, high order compact scheme, hermitian scheme, collocation method, Mehrstellenverfahren, mixed method, elliptic problems

1 Introduction

The purpose of this paper is to introduce a hermitian box-scheme for elliptic problems in conservative form, with interesting accuracy properties, especially for the gradient of the solution.

The scheme we present is apparently new. It is defined on a regular finite difference grid, but its design applies also to a non equispaced grid. The design borrows ingredients to:

*This work has been performed with the support of the GDR MOMAS, (ANDRA, CEA, EDF, BRGM and CNRS): *Modélisation pour le stockage des déchets radioactifs.* The author thanks especially A. Bourgeat for his encouragements and his interest in this work.

- The box-scheme of Keller [20], in the setting of [13].
- The hermitian interpolation of the gradient, which is introduced in Collatz, [9]. That kind of interpolation is the basis of the so-called compact schemes, [21], [15].
- The Stephenson scheme for the biharmonic problem, introduced in [28], which has been recently used for the numerical simulation of the incompressible time-dependent Navier-Stokes equations, [4], [3].

Briefly, we consider as in most of the methods for elliptic problems, a scheme in mixed form, but we consider the mixed form on the "box" a lenght $2h$, $K_j = [x_{j-1}, x_{j+1}]$. As in [13], we take the average of the conservation law and of the constitutive law. Therefore, the resulting scheme has a finite-volume design, but with overlapping volumes. A difference with methods like the mixed finite element method, [27], the control volume method, [8], or so-called box-methods, [17, 19], is that our box-scheme is not parameter free. As in [12, 14, 16], we have to adjust locally in each box the accuracy of the quadrature rule for the gradient. The main properties of the hermitian box-scheme are:

- Fourth order accuracy for $p = u'(x)$ and $u(x)$ on regular problems at interior points, with a convergence rate of 1.5 for regular problems. We observe even in many cases a superconvergence rate for the gradient.
- A very good capability to handle sharp contrasts in the diffusion coefficients. We observe a practical convergence rate in the H^1 norm ranging from 1 to 2.5, for 1D problems with contrasts up to 10^4 in the ellipticity.
- A great flexibility in the design, permitted by the variation of the quadrature rule for the gradient.

The outline of the paper is as follows. After the notation in Section 2, we describe in Section 3 the design principles of the scheme on the 1D Poisson problem. In Section 4, we precise the connection with a non standard finite element method and give some error estimates. The scheme appears to be 4rd order in u and p. In Section 5, we focus on numerical tests in 1D. First we observe a remarkable superconvergence of the gradient for regular solutions. The scheme behaves very well, even on coarse grids, with very good error levels. Then, we apply the hermitian-box scheme to several numerical tests for problems with high contrasts in the diffusion coefficients, originating from the test suite in [24]. That kind of problems is still of high interest in the porous media community, where the accurate computation of the fluid velocity flows in fractured and layered soils is an important question. In addition the numerical analysis of methods for such problems has recently

been adressed in [24], [2], [29].
Finally, let us insist on the fact that the design of the present scheme is connected with the compact scheme collocation methodology [9], [21], [28]. See also [6] for another collocation scheme. The numerical analysis is also tractable using the formalism of the mixed finite element method, [1, 7, 23, 5, 12].

2 Finite differences and finite elements notation

We consider for $f \in L^2[0,1]$ the linear 1D elliptic problem in $[0,1]$

$$\begin{cases} -(k(x)u_x)_x = f(x) \quad , \quad 0 < x < 1 \\ u\,(0) = 0, \quad u\,(1) = 0, \end{cases} \tag{1}$$

where $k(x) > 0$ is a piecewise continuous ellipticity function on $[0,1]$. This problem is well-posed in $H_0^1(]0,1[)$, which means in particular that $u(x)$ is continuous and that $u_x(x) \in L^2(0,1)$. In addition, any solution of the homogeneous equation

$$-(k(x)u_x)_x = 0 \quad , \quad 0 < x < 1. \tag{2}$$

verifies the maximum principle, that is, it attains its extremal values in α or β, see for example [26]. We consider the discretisation of (1) on a regular finite difference grid $x_1 = 0 < x_2 < ... < x_{N-1} < x_N = 1$ with grid-size h. We denote by l_h^2 the space of sequences u_j, $1 \leq j \leq N$ and $l_{h,0}^2$ the subspace of sequences with $u_1 = u_N = 0$. We note the scalar product and the norm on l_h^2

$$(u,v)_h = h\sum_{j=1}^{N} u_j v_j \quad , \quad |u|_h^2 = h\sum_{j=1}^{N} u_j^2. \tag{3}$$

We denote also the equivalent scalar product and norm on l_h^2 defined by

$$(u,v)_{h'} = \frac{h}{2}u_1v_1 + h\sum_{j=2}^{N-1} u_j v_j + \frac{h}{2}u_N v_N \quad , \quad |u|_{h'}^2 = \frac{h}{2}u_1^2 + h\sum_{j=2}^{N-1} u_j^2 + \frac{h}{2}u_N^2. \tag{4}$$

The relation (4) corresponds to the trapezoidal quadrature rule on the interval $I = [0,1]$, [18]. The grid function $\varphi^i \in l_h^2$ is the canonical basis of l^2 defined by $\varphi_j^i = \delta_{i,j}$ (Kronecker symbol).
We denote as usual the operators δ_x^2, δ_x, $\delta_x^{\pm}$,

$$\begin{cases} \delta_x^2 u_j = \dfrac{u_{j+1} + u_{j-1} - 2u_j}{h^2} \quad ; \quad \delta_x u_j = \dfrac{u_{j+1} - u_{j-1}}{2h} \quad , \quad 2 \leq j \leq N-1 \\ \delta_x^+ u_j = \dfrac{u_{j+1} - u_j}{h} \quad , \quad 1 \leq j \leq N-1 \quad ; \quad \delta_x^- u_j = \dfrac{u_j - u_{j-1}}{h} \quad , \quad 2 \leq j \leq N. \end{cases} \tag{5}$$

We extend each definition in (5) to a boundary point $j_0 = 1$ or N, when needed, by $\delta_x^2 u_{j_0} = \delta_x u_{j_0} = \delta_x^{\pm} u_{j_0} = 0$.
The discrete integration by parts formulas are, for all $u, v \in l^2_{h,0}$

$$\begin{array}{l} \bullet \quad (\delta_x^2 u, v)_h = -(\delta_x^- u, \delta_x^- v)_h = -(\delta_x^+ u, \delta_x^+ v)_h, \\ \bullet \quad (\delta_x^+ u, v)_h = -(u, \delta_x^-, v)_h. \end{array} \tag{6}$$

We introduce also for all $u \in l^2_h$, the following operator

$$\widetilde{\delta}_x u_j = \begin{cases} \delta_x^+ u_1 \ , & j = 1, \\ \delta_x u_j \ , & 2 \le j \le N-1, \\ \delta_x^- u_N \ , & j = N. \end{cases} \tag{7}$$

Finally $|\delta_x^+ u|_h$ and $|\widetilde{\delta}_x u|_{h'}$ are norms on $l^2_{h,0}$ and we have the following discrete Poincaré inequalities.

Lemma 2.1 (Discrete Poincaré inequalities) *(i) For all $u \in l^2_{h,0}$, we have*

$$|u|_h \le 2|\delta_x^+ u|_h, \tag{8}$$

(ii) For all $u \in l^2_{h,0}$, we have

$$|u|_h \le 4|\widetilde{\delta}_x u|_{h'}. \tag{9}$$

Proof: (i) see e.g. [3].
(ii) Suppose $u \in l^2_{h,0}$. It is easy to verify that (consider separately the cases i_0 odd and i_0 even) that

$$u_{i_0}^2 \le 4|\widetilde{\delta}_x u|_{h'}|u|_h, \quad i_0 = 1, .., N. \tag{10}$$

Since $h = \frac{1}{N-1}$, we have for all $u \in l^2_{h,0}$

$$|u|_h^2 = \sum_{i=2}^{N-1} h u_i^2 \le 4\frac{N-2}{N-1}|\widetilde{\delta}_x u|_{h'}|u|_h. \tag{11}$$

which gives (9). ■
To each grid functions $u \in l^2_{h,0}$, $p \in l^2_h$, we match their corresponding piecewise linear finite element functions called $u_h(x)$, $p_h(x)$, defined by

$$u_h(x) = \sum_{j=2}^{N-1} u_j \varphi_h^j(x) \ \ , \ \ p_h(x) = \sum_{j=1}^{N} p_j \varphi_h^j(x). \tag{12}$$

In particular, $\varphi_h^j(x)$ is the "hat" function associated to point x_j, matched to the grid function φ^j. A grid function in $l^2_{h,0}$ corresponds to a finite element function in the space $P^1_{c,0} = \mathrm{Span}(\varphi_2, ..., \varphi_{N-1})$. For $u_h \in P^1_c$,

$\bar{u}_h \in P^0$ is the piecewise constant function defined in $[x_j, x_{j+1}]$ by $u_{j+1/2} = (u_j + u_{j+1})/2$. A grid function in l_h^2 corresponds to a finite element function in $P_c^1 = \text{Span}(\varphi_1, ..., \varphi_N)$. Finally, we denote the L^2 scalar product in $[0,1]$ by (f,g), the L^2 norm by $|f|$, and the L^∞ norm by $|f|_\infty$.
We begin by the following lemma, [3].

Lemma 2.2 *The following identities hold*
(i) For all $u, v \in l_h^2$,

$$(u,v)_{h'} = (u_h, v_h) + \frac{h^2}{6}(u_{h,x}, v_{h,x}) = (\bar{u}_h, \bar{v}_h) + \frac{h^2}{4}(u_{h,x}, v_{h,x}). \tag{13}$$

In particular, if $u \in l_{h,0}^2$ *or* $v \in l_{h,0}^2$*, the left hand side of (13) is* $(u,v)_h$.
(ii) For all $u, v \in l_h^2$,

$$(\widetilde{\delta}_x u, v)_{h'} = (u_{h,x}, v_h) = -(u, \widetilde{\delta}_x v)_{h'} + u_N v_N - u_1 v_1. \tag{14}$$

In particular, if $u \in l_{h,0}^2$ *or* $v \in l_{h,0}^2$,

$$(\widetilde{\delta}_x u, v)_{h'} = (u_{h,x}, v_h) = -(u_h, v_{h,x}) = -(u, \widetilde{\delta}_x v)_{h'}. \tag{15}$$

(iii) For all $u, v \in l_{h,0}^2$*, we have*

$$(\delta_x^2 u, v)_h = -(u_{h,x}, v_{h,x}). \tag{16}$$

(iv) For all $p \in l_h^2$*, with* $p_h \in P_c^1$ *the matching finite element function, we have*

$$|p_{h,x}| \leq \frac{2}{h}|p|_{h'}. \tag{17}$$

Proof:
The proofs are elementary computations resulting from the fact that u_h is piecewise linear and $u_{h,x}$ piecewise constant in each cells $K_{j+1/2} = [x_j, x_{j+1}]$. ■

In the sequel, we use the following notation

- $u(x)$ is the exact solution of (19) and $p(x) = u'(x)$ is its derivative (the flux).
- $\tilde{u} \in l_{h,0}^2$, $\tilde{p} \in l_h^2$ are the grid functions defined by the interpolated values

  $$\tilde{u}_j = u(x_j) \ \ , \ \ \tilde{p}_j = p(x_j) \ \ , \ \ 1 \leq j \leq N. \tag{18}$$

  We note also $\tilde{u}_h \in P_{c,0}^1$, $\tilde{p}_h \in P_c^1$ the matched finite elements functions respectively to $\tilde{u}$, $\tilde{p}$.
- $u \in l_{h,0}^2$, $p \in l_h^2$ are the discrete solutions of the hermitian box-scheme, see Section 3.

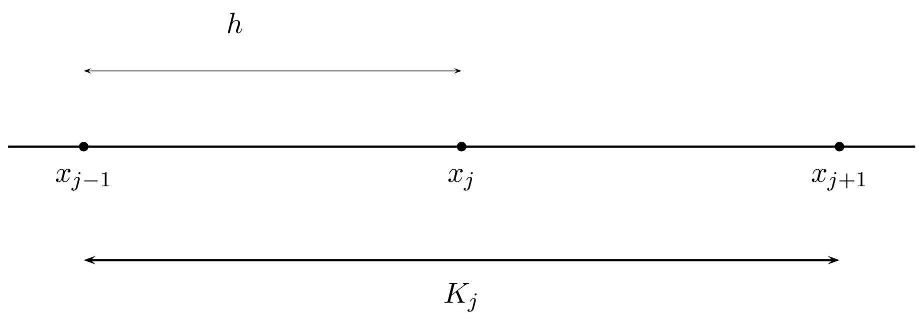

Figure 1: *The stencil of the hermitian box-scheme:* $K_j = [x_{j-1}, x_{j+1}]$

3 A hermitian box-scheme for the 1-D elliptic problem

3.1 Definition of the scheme

We introduce here the general principle of the hermitian box-scheme on the simple model of the one-dimensional Poisson problem:

$$\left\{ \begin{array}{ll} -u_{xx}(x) = f(x) \quad , \quad 0 < x < 1 \ , & (a) \\ u(0) = 0 \qquad , \qquad u(1) = 0 \quad (b). & \end{array} \right. \tag{19}$$

As in the case of the standard box-scheme, the design of the hermitian box-scheme for (19) is in two steps, [20, 10, 11, 12, 13]. First, (19) is recasted in mixed form

$$\left\{ \begin{array}{ll} p_x + f = 0 & (a) \\ p - u_x = 0 & (b) \\ u(0) = u(1) = 0 & (c). \end{array} \right. \tag{20}$$

We consider now "boxes" constitued of the cells $K_j = [x_{j-1}, x_{j+1}]$, see Fig 3.1. In contrast with [13], the boxes K_j, K_{j+1} overlap, $K_j \cap K_{j+1} = [x_j, x_{j+1}]$. Suppose that $u(x)$ is an exact C^1 solution of (19) and $p(x) := u'(x)$ is its gradient. We take the average of (20_a) and (20_b) on the boxes K_j, for all $2 \le j \le N-1$ which gives that the exact solution $(u, p = u_x)$ verifies the $2(N-1)$ equations

$$\left\{ \begin{array}{l} p(x_{j+1}) - p(x_{j-1}) = -2h\,(\Pi^0 f)_{|j} \ \ , 2 \le j \le N-1 \quad (a) \\ 2h\,(\Pi^0 p)_{|j} - [u(x_{j+1}) - u(x_{j-1})] = 0 \ \ , 2 \le j \le N-1 \quad (b) \\ u(x_1) = u(x_N) = 0 \quad (c). \end{array} \right. \tag{21}$$

In (21), Π^0 stands for the average operator on the box $K_j = [x_{j-1}, x_{j+1}]$, that is, for any function $g(x)$,

$$(\Pi^0 g)_j = \frac{1}{2h} \int_{x_{j-1}}^{x_{j+1}} g(x) dx. \tag{22}$$

Furthermore, in order to have a set of $2N$ equations corresponding to the $2N$ values $(u(x_j), p(x_j))$, we have to consider some definition of the values of $p(x_1)$, $p(x_N)$. Suppose we complete the system (21) by the two equations giving the derivatives $p_1 = u'(0)$, $p_N = u'(1)$ as functions of $f(x)$. Then, the exact solution u of the continuous problem (19), and its gradient p satisfy the following system of equations

$$\begin{cases} p\left(x_{j+1}\right) - p\left(x_{j-1}\right) = -2h\left(\Pi^0 f\right)_{|j} \quad (a) \\ 2h\left(\Pi^0 p\right)_{|j} - \left[u\left(x_{j+1}\right) - u\left(x_{j-1}\right)\right] = 0 \quad (b) \\ u\left(x_1\right) = u\left(x_N\right) = 0 \quad (c) \\ p(0) = u'(0) \;\; (d) \\ p(1) = u'(1) \;\; (e). \end{cases} \tag{23}$$

In the case of problem (19), the exact solution is explicitely given in function of $f(x)$ by

$$u(x) = x\int_0^1 (1-s)f(s)ds - \int_0^x (x-s)f(s)ds \quad , \quad p(x) = \int_x^1 f(s)ds - \int_0^1 sf(s)ds, \tag{24}$$

so that $p(0) = u'(0)$ and $p(1) = u'(1)$, are

$$\begin{cases} p(0) = \displaystyle\int_0^1 (1-s)f(s)ds \\ p(1) = -\displaystyle\int_0^1 sf(s)ds. \end{cases} \tag{25}$$

We now deduce from (23) a finite difference scheme in (u_j, p_j) with $u_j \simeq \tilde{u}_j$, $p_j \simeq \tilde{p}_j$, by specifying the two following approximations

- *Approximation of the average of the flux* $\Pi^0 p_j$.
- *Approximation of the boundary operator* $f \mapsto (u_x(0), u_x(1))$.

Suppose that $2 \leq j \leq N$. The average of the flux on $K_j = [x_{j-1}, x_{j+1}]$ is

$$\Pi^0 p_j = \frac{1}{2h}\int_{x_{j-1}}^{x_{j+1}} p(t)dt. \tag{26}$$

We approximate $\Pi^0 p_j$ by the Simpson formula

$$P_S p_j = \frac{1}{6}p_{j-1} + \frac{2}{3}p_j + \frac{1}{6}p_{j+1} \simeq \Pi^0 p_j. \tag{27}$$

Note that the relation (27), which is characteristic of the cubic splines interpolation, see [25], [18], is also used to define the gradient in the Stephenson scheme for the biharmonic problem, [28], [4], [3]. Recall that the error representation of Simpson formula is given by the Peano Kernel Theorem, [18].

$$\Pi^0 p_j - P_S p_j = \frac{1}{2h}\int_{-h}^{h} K_S(\sigma)p^{(4)}(x_j + \sigma)d\sigma, \tag{28}$$

where $K_S(t)$ is the negative function defined for $|t| \leq h$ by

$$K_S(t) = -\frac{1}{72}(h-|t|)^3(h+3|t|). \tag{29}$$

Note that in (28), we can replace $p^{(4)}$ by $-f^{(3)}$. Suppose we extend the function $u(x)$ by imparity on $[-h,0]$, so that the function $p(x)$ is extended by parity. If the function $p(x)$ defined in that way is C^4 on $[-h,h]$, which is equivalent to the fact that $p'(0) = p'''(0) = 0$, then formula (28) holds for $j=1$ on $[-h,h]$. Since the kernel $K_S(\sigma)$ satifies $K_S(\sigma) = K_S(-\sigma)$, where the Simpson operator P_S is extended at $j=1$ by

$$P_S p_1 = \frac{2}{3}p_1 + \frac{1}{3}p_2 \simeq \frac{1}{h}\int_{x_1}^{x_2} p(t)dt. \tag{30}$$

Similarly, $P_S p_N$ is defined at $x_N = 1$ by

$$P_S p_N = \frac{2}{3}p_N + \frac{1}{3}p_{N-1} \simeq \frac{1}{h}\int_{x_{N-1}}^{x_N} p(t)dt. \tag{31}$$

In general however, we do not have that p is C^4 on $[-h,h]$, so that we only have at $x_1 = 0$ the simple formula, also obtained by the Kernel Peano Theorem

$$\int_{x_1}^{x_2} p(t)dt = h(\frac{2}{3}p_1 + \frac{1}{3}p_2) + \int_0^h (\frac{2}{3}h - \sigma)p'(x_1+\sigma)d\sigma, \tag{32}$$

and at $x_N = 1$,

$$\int_{x_{N-1}}^{x_N} p(t)dt = h(\frac{2}{3}p_N + \frac{1}{3}p_{N-1}) - \int_{-h}^0 (\frac{2}{3}h + \sigma)p'(x_N+\sigma)d\sigma. \tag{33}$$

We denote by $k^S \in l_h^2$ the grid function defined for the exact solution $p(x)$ by

$$k_j^S = \begin{cases} (\Pi^0 p)_j - P_S p_j = \dfrac{1}{2h}\displaystyle\int_{-h}^{h} K_S(\sigma)p^{(4)}(x_j+\sigma)d\sigma \ \ , \ \ 2 \leq j \leq N-1, \\ \dfrac{1}{h}\displaystyle\int_{x_1}^{x_2} p(t)dt - (P_S p)_1 = \dfrac{1}{h}\displaystyle\int_0^h (\dfrac{2}{3}h - \sigma)p'(x_j+\sigma)d\sigma \ \ , \ \ j = 1, \\ \dfrac{1}{h}\displaystyle\int_{x_{N-1}}^{x_N} p(t)dt - P_S p_N = -\dfrac{1}{h}\displaystyle\int_{-h}^0 (\dfrac{2}{3}h + \sigma)p'(x_j+\sigma)d\sigma \ \ , \ \ j = N. \end{cases} \tag{34}$$

We deduce from (34)

$$|k_j^S| \leq \frac{1}{180}h^4|p^{(4)}|_{\infty,[0,1]} \ \ , \ \ |k_1^S| \leq \frac{5}{18}h|p'|_{\infty,[0,h]} \ \ , \ \ |k_N^S| \leq \frac{5}{18}h|p'|_{\infty,[1-h,1]}. \tag{35}$$

Now, the exact grid solution $\tilde{u}_j$, $\tilde{p}_j$ verifies at interior points $2 \le j \le N-1$,

$$\delta_x \tilde{u}_j = \Pi^0 p_j = \frac{1}{2h} \int_{x_{j-1}}^{x_{j+1}} p(x)dx = P_S \tilde{p}_j + k_j^S. \tag{36}$$

At point $x_1 = 0$, we have

$$\delta_x^+ \tilde{u}_1 = \frac{1}{h} \int_{x_1}^{x_2} p(x)dx = \frac{1}{3}\tilde{p}_1 + \frac{2}{3}\tilde{p}_2 + k_1^S = P_S \tilde{p}_1 + k_1^S, \tag{37}$$

and at point $x_N = 1$,

$$\delta_x^- \tilde{u}_N = \frac{1}{h} \int_{x_{N-1}}^{x_N} p(x)dx = \frac{1}{3}\tilde{p}_{N-1} + \frac{2}{3}\tilde{p}_N + k_N^S = P_S \tilde{p}_N + k_N^S. \tag{38}$$

We deduce from (36, 37, 38) that

$$P_S \tilde{p}_j = \widetilde{\delta}_x \tilde{u}_j - k_j^S \ \ , \ \ 1 \le j \le N. \tag{39}$$

The *Hermitian Box Scheme* (referred in the sequel as HB scheme) for the Poisson problem (20) reads now: Find $U = [u_1, u_2, ...u_{N-1}, u_N] \in l_h^2$, $P = [p_1, p_2, ...p_{N-1}, p_N] \in l_h^2$ solution of

$$\begin{cases} -\dfrac{p_{j+1} - p_{j-1}}{2h} = \Pi^0 f_j \ \ , \ \ 2 \le j \le N-1 \quad (a) \\ \dfrac{1}{6}p_{j-1} + \dfrac{2}{3}p_j + \dfrac{1}{6}p_{j+1} = \delta_x u_j \ \ , \ \ 2 \le j \le N-1 \quad (b) \\ u_1 = u_N = 0 \quad , \quad \text{(Dirichlet conditions)} \quad (c) \\ \dfrac{1}{3}p_2 + \dfrac{2}{3}p_1 = \dfrac{1}{h}(u_2 - u_1) \quad (d) \\ \dfrac{1}{3}p_{N-1} + \dfrac{2}{3}p_N = \dfrac{1}{h}(u_N - u_{N-1}) \quad (e). \end{cases} \tag{40}$$

Observe that $(40)_{(b),(d),(e)}$ can be rewritten as

$$P_S p = \widetilde{\delta}_x u, \tag{41}$$

Finally the HB scheme rewrites: find $(u, p) \in l_{h,0}^2 \times l_h^2$ solution of

$$\textbf{HB scheme} \begin{cases} -\delta_x p_j = \Pi^0 f_j \ \ , \ \ 2 \le j \le N-1 \quad (a') \\ (P_S p)_j = \widetilde{\delta}_x u_j \ \ , \ \ 1 \le j \le N \quad (b'). \end{cases} \tag{42}$$

Lemma 3.1 *(i) The relation $(42)_{b'}$ is 4th order in the finite difference sense at the interior points $2 \le j \le N-1$. (Note that the relation $(42)_{a'}$ is exact for all $j = 2, .., N-1$).*
(ii) The application $u \in l_{h,0}^2 \mapsto |p|_{h'}$ with $p \in l_h^2$ defined by $(42)_{b'}$ defines a norm on $l_{h,0}^2$ and there exist constants C_1, C_2 such that

$$C_1 |\widetilde{\delta}_x u|_{h'} \le |p|_{h'} \le C_2 |\widetilde{\delta}_x u|_{h'}. \tag{43}$$

Proof: (i) has been proved in (35).
(ii): The grid function $p \in l_h^2$ is defined from $u \in l_{h,0}^2$ by

$$P_S p = \widetilde{\delta}_x u. \tag{44}$$

The Simpson operator P_S in (44) can be written

$$P_S = I + B, \tag{45}$$

where B is defined by

$$Bp_j = \begin{cases} \dfrac{h}{3}\delta_x^+ p_1 \ \ , \ \ j = 1 \\ \dfrac{h^2}{6}\delta_x^2 p_j \ \ , \ \ 2 \leq j \leq N-1 \\ -\dfrac{h}{3}\delta_x^- p_N \ \ , \ \ j = N. \end{cases} \tag{46}$$

We have clearly $\|B\|_\infty \leq 2/3$, therefore

$$\|B\|_{h'} = \sup_{q \in l_h^2, q \neq 0} \frac{|Bq|_{h'}}{|q|_{h'}} \leq \frac{2}{3}. \tag{47}$$

The inverse of P_S is given in $\mathcal{L}(l_{2,h})$ by the Neumann series

$$P_S^{-1} = \sum_{n=0}^{+\infty} (-1)^{n-1} B^n, \tag{48}$$

which gives

$$\|P_S^{-1}\|_{h'} \leq \sum_{n \geq 0} \big(\frac{2}{3}\big)^n = 3, \tag{49}$$

and

$$p = P_S^{-1} \widetilde{\delta}_x u. \tag{50}$$

Therefore we have

$$\frac{1}{\|P_S\|_{h'}} |\widetilde{\delta}_x u|_{h'} \leq |p|_{h'} \leq \|P_S^{-1}\|_{h'} |\widetilde{\delta}_x u|_{h'}, \tag{51}$$

which gives (43). ■

At this point, one may wonder if the grid gradient u_x cannot be eliminated in a simple way and if the scheme (42) is not an already known scheme.

Lemma 3.2 *The HB scheme (42) is equivalent to the scheme*

$$-\left[(\delta_x \circ P_S^{-1} \circ \widetilde{\delta}_x)u\right]_j = (\Pi^0 f)_j \quad , \quad 2 \le j \le N-1. \tag{52}$$

completed with the implicit recovery of the gradient (50). The scheme (52) is 4th order in u. In addition, for $j = 2, ..., N-1$, relation (52) rewrites

$$-\frac{u_{j+2} + u_{j-2} - 2u_j}{4h^2} = \frac{1}{6}\Pi^0 f_{j-1} + \frac{2}{3}\Pi^0 f_j + \frac{1}{6}\Pi^0 f_{j+1}, \tag{53}$$

with the convention that $u_0 = -u_2$, $(\Pi^0 f)_1 = 0$, and $u_{N+1} = -u_{N-1}$, $(\Pi^0 f)_N = 0$.

Proof: Using (50), we observe that the HB scheme (42) can be expressed in u only by: find $u \in l^2_{h,0}$ solution of

$$-\left[(\delta_x \circ P_S^{-1} \circ \widetilde{\delta}_x)u\right]_j = (\Pi^0 f)_j \quad , \quad 2 \le j \le N-1. \tag{54}$$

This expression is not explicit, since we have to invert the Simpson matrix P_S. Once $u \in l^2_{h,0}$ is known, $p \in l^2_h$ is recovered by (50). The symbol $a(\theta)$, for all semi-discrete Fourier mode $\theta = h\xi \in [0, 2\pi[$, of the operator

$$u_j \mapsto \Pi^0(u'')_j - \left[(\delta_x \circ P_S^{-1} \circ \widetilde{\delta}_x)u\right]_j \tag{55}$$

is

$$a(\theta) = -\xi^6 \frac{h^4}{180} + O(h^6), \tag{56}$$

which proves that (53) is actually 4th order in u (in the periodic setting). Observe now that at any interior point j, $2 \le j \le N-1$,

$$\begin{cases} -\delta_x p_j = \Pi^0 f_j \quad , \quad 2 \le j \le N-1 \quad (a) \\ (I + \dfrac{h^2}{6}\delta_x^2)p_j = \delta_x u_j \quad , \quad 2 \le j \le N-1 \quad (b). \end{cases} \tag{57}$$

Applying δ_x on each side of $(57)_b$, we find, (note that $\delta_x \circ \delta_x^2 = \delta_x^2 \circ \delta_x$),

$$\delta_x(I + \frac{h^2}{6}\delta_x^2)p_j = \delta_x(\delta_x u)_j. \tag{58}$$

Therefore

$$(I + \frac{h^2}{6}\delta_x^2)\delta_x p_j = \delta_x(\delta_x u)_j \quad , \tag{59}$$

and using $(57)_a$, one obtains that u_j is solution of the following scheme

$$-\delta_x(\delta_x)u_j = (I + \frac{h^2}{6}\delta_x^2)(\Pi^0 f)_j \quad , \quad 3 \le j \le N-2. \tag{60}$$

which is (53). Furthermore, the same computation is valid for $j = 2$, $j = N-1$, according to the extension by imparity of u_j and $f(x)$ at $x = 0$, $x = 1$. ■

Remark 1:
On can replace in (52) the integral of $f(x)$ over K_j by any 4th order quadrature formula, in order to preserve the 4th order accuracy. For example, if the Simpson rule is used, we obtain for $j = 3, .., N-3$ the scheme

$$-\frac{u_{j+2} + u_{j-2} - 2u_j}{4h^2} = \frac{1}{36}f_{j-2} + \frac{2}{9}f_{j-1} + \frac{1}{2}f_j + \frac{2}{9}f_{j+1} + \frac{1}{36}f_{j+2}. \quad (61)$$

Remark 2:
Recall that a standard 4th order finite difference scheme is the MV[1] scheme of Collatz, [9], defined by

$$-\frac{u_{j+2} + u_{j-2} - 2u_j}{4h^2} = \frac{1}{12}f_{j-2} + \frac{5}{6}f_j + \frac{1}{12}f_{j+2}. \quad (62)$$

Observe that the MV scheme (62) and the HB scheme (53) differ only by the interpolation operator applied to the source term. It appears that the two schemes are different and both of order 4. The usual derivation of the MV scheme, [9], is obtained by collocation for the unknown u alone. The flux p is not involved. In addition, the MV scheme has to be supplied with a lower order scheme at the 2 near boundary points. In the contrary, the 4th order approximation of the gradient is provided by the HB scheme in a consistent way.

Remark 3:
The stability result obtained in (43), is due to the boundary condition on p approximating the boundary operator. Note however, that this stability result cannot *a priori* ensure the absence of oscillations. Actually, the form (60) suggests a possible decoupling odd/even. Therefore, in the "far field", the scheme associated with the operator $\delta_x \circ \delta_x$ uses only odd (or even) points, which could give oscillations.

Remark 4:
Note finally that the global conservativity in the scheme (42) is clear only when there is an even number of cells $[x_{j-1}, x_j]$, i.e. an odd number of points.

4 Numerical analysis

4.1 Error estimate

In this section, we show, how the finite element analogy of the finite difference setting can help to perform the numerical analysis.

[1] Mehrstellenverfahren

Let us begin by the finite element interpretation of the hermitian relation connecting the grid gradient function $p \in l^2_h$ of $u \in l^2_{h,0}$ with the gradient of the finite element function $u_h(x) \in P^1_{c,0}$ matching u.

Lemma 4.1 *The hermitian relation $(42)_{b'}$ is equivalent to the fact that p_h is the orthogonal L^2 projection of $u_{h,x}$ on P^1_c, that is,*

$$(p_h - u_{h,x}, q_h) = 0 \ \ , \ \ \forall q_h \in P^1_c. \tag{63}$$

Proof:
The proof is straightforward considering separately the case $q_h \in P^1_{c,0}$ which corresponds to $(40)_b$ and $q_h = \varphi^1_h, \varphi^N_h$ which corresponds to $(40)_{b,d}$. Note that the Simpson operator translates simply in the finite element language as the mass matrix. ■

Theorem 4.1 *(i) There exists a unique solution $(u,p) \in l^2_{h,0} \times l^2_h$ solution of (40) satisfying*

$$|u|_h + |p|_{h'} \leq C|f|_{L^2[0,1]}. \tag{64}$$

(ii) The following error estimate between the grid interpolated values of the exact solution $\tilde{u}_j = u(x_j)$, $\tilde{p}_j = p(x_j)$, and the solution (u,p) of the scheme (42) holds

$$|\tilde{u} - u|_h + |\tilde{p} - p|_{h'} \leq C\left[h^{3/2}|f|_{\infty,[0,h]\cup[1-h,1]} + h^4|f^{(3)}|_{\infty,[0,1]}\right]. \tag{65}$$

Proof: We use for the stability estimate (64) the finite element analogy, and for (ii) a direct proof.
(i) We have that $p \in l^2_h$ verifies

$$-\delta_x p_j = (\Pi^0 f)_j \quad 2 \leq j \leq N-1. \tag{66}$$

This is equivalent to the fact that for all $v \in l^2_{h,0}$,

$$\begin{aligned}(\Pi^0 f, v)_h &= -(\delta_x p, v)_h = -(\widetilde{\delta}_x p, v)_{h'} = (p, \widetilde{\delta}_x v)_{h'} = (p_h, v_{h,x}) \\ &= (p_h, v_{h,x} - q_h) + (p_h, q_h) = (p_h, q_h).\end{aligned}$$

Taking $q_h = p_h$, and therefore $v = u$, we obtain

$$|p_h|^2 \leq |\Pi^0 f|_h |u|_h. \tag{67}$$

The left-hand side is bounded from above, by, (see (13), (17)),

$$|p_h|^2 \geq |p|^2_{h'} - \frac{h^2}{6}|p_{h,x}|^2 \geq (1 - \frac{2}{3})|p|^2_{h'} = \frac{1}{3}|p|^2_{h'} \tag{68}$$

Using (17), we obtain finally

$$|p_h|^2 \geq (1-\frac{2}{3})|p|^2_{h'} = \frac{1}{3}|p|^2_{h'}. \tag{69}$$

On the right-hand-side, we have by (9), (P_S is the Simpson operator defined in (28,30,31)),

$$|u|_h \leq C|\widetilde{\delta}_x u|_{h'} \leq C\|P_S\|_{h'}|p|_{h'}. \tag{70}$$

Combining (67), (68), (69), we obtain, (C is a generic constant)

$$|p|_{h'} \leq C|\Pi^0 f|_h, \tag{71}$$

and (64) follows from

$$|u|_h \leq C|\widetilde{\delta}_x u|_{h'} \leq C'|p|_{h'}. \tag{72}$$

In particular, (40) has a unique solution, since $f \equiv 0$ gives $\Pi^0 f \equiv 0$ therefore $p \equiv 0$ and $u \equiv 0$ by (64).
(ii) We note $e^u = \tilde{u} - u \in l^2_{h,0}$, $e^p = \tilde{p} - p \in l^2_h$, respectively the grid error functions for u and p. For all $v \in l^2_h$, we have by (13),

$$(\widetilde{\delta}_x e^u, v)_{h'} = -(e^u, \widetilde{\delta}_x v)_{h'}. \tag{73}$$

Choosing the test function $v = e^p \in l^2_h$ as the error on p, we have

$$(\widetilde{\delta}_x e^u, e^p)_{h'} = -(e^u, \widetilde{\delta}_x e^p)_{h'}. \tag{74}$$

But, due to the fact that $\delta_x p_j = \delta_x \tilde{p}_j = -\Pi^0 f_j$, $j = 2,..N-1$, we have $\widetilde{\delta}_x e^p_j = 0$, $j = 2,...N-1$. Furthermore, since $e^u_1 = e^u_N = 0$, we deduce

$$(e^u, \widetilde{\delta}_x e^p)_{h'} = 0 \quad , \tag{75}$$

and therefore

$$(\widetilde{\delta}_x e^u, e^p)_{h'} = 0. \tag{76}$$

Now, we deduce from (42), that the error $e^u = \tilde{u} - u$ verifies in l^2_h,

$$\widetilde{\delta}_x e^u = \widetilde{\delta}_x \tilde{u} - \widetilde{\delta}_x u = P_S \tilde{p} + k^S - P_S p = P_S e^p + k^S, \tag{77}$$

therefore, by (76),

$$(P_S e^p, e^p)_{h'} = (\widetilde{\delta}_x e^u, e^p)_{h'} - (k^S, e^p)_{h'} = -(k^S, e^p)_{h'}. \tag{78}$$

On the left-hand side, we have

$$C|e^p|^2_{h'} \leq C|e^p_h|^2 \leq (P_S e^p, e^p)_{h'}, \tag{79}$$

and the right-hand-side is estimated by

$$|(k^S, e^p)_{h'}| \le |k^S|_{h'} |e^p|_{h'}. \tag{80}$$

Using (35), we find

$$|k^S|_{h'} \le C\left[h^{3/2}|f|_{\infty,[0,h]\cup[1-h,1]} + h^4|f^{(3)}|_{\infty,[0,1]}\right], \tag{81}$$

where the first term in the r.h.s. of (81) is due to the 2 boundary points and the other term is due to the interior points $j = 2, .., N-2$. Finally,

$$|\tilde{p} - p|_{h'} = |e^p|_{h'} \le |k^S|_{h'}. \tag{82}$$

Coming back to (77), the error on u is estimated by

$$\widetilde{\delta}_x e^u = P_S e^p + k^S, \tag{83}$$

we obtain

$$|\widetilde{\delta}_x e^u|_{h'} \le |P_S e^p|_{h'} + |k^S|_{h'} \le \|P_S\|_{h'} |e^p|_{h'} + |k^S|_{h'} \le |e^p|_{h'} + |k^S|_{h'}, \tag{84}$$

and (65) results from (82, 81,84) and the Poincaré inequality (9). ■

Note that the consistency error at interior points is 4. The loss of accuracy comes from the boundary conditions. However, that loss of accuracy is also the origin of the stability of the scheme. We do not investigate further alternative quadrature rules for p as well as other boundary conditions, because Simpson rule has given good results so far. Note that the error e_j^p in p takes only two values, one for j odd, and one for j even.

4.2 Mixed Finite Element interpretation

In this section, we show the mixed finite element form of the HB scheme (42). We refer to [1], [7], [23] for classical references on that type of methods.

This form is non-standard and one has to use the unknowns $(u_h, p_h) \in P^1_{c,0} \times P^1_c$. If $v_h \in P^1_{c,0}$ is any test function, we call $q_h \in P^1$ the gradient of v_h in the sense of (63), that is the projection of v_h on the space of P^1 functions.

In the two following propositions, we summarize simple facts on the finite element formulation of scheme (42).

The Hilbert spaces are

- $u \in H^1_0(]0,1[)$, equipped with the norm $|u|_1 = |u_x|_{L^2(0,1)}$.
- $p \in L^2(0,1)$, equipped with the norm $|p| = |p|_{L^2(0,1)}$.

and the variational formulation of the Poisson problem is: find $(u,p) \in H_0^1 \times L^2$ solution of

$$\begin{cases} (p, v_x) = (f, v) \ ; \ \forall v \in H_0^1 \quad , \\ (p - u_x, q) = 0 \ ; \ \forall q \in L^2. \end{cases} \tag{85}$$

We have a conforming approximation,

$$u_h \in P_{c,0}^1 \subset H_0^1 \ , \ p_h \in P_c^1 \subset L^2. \tag{86}$$

We denote for all $f \in L^2[0,1]$,

- The grid function $(\Pi^0 f)_j \in l_{h,0}^2$ defined by

$$(\Pi^0 f)_j = \frac{1}{2h} \int_{x_{j-1}}^{x_{j+1}} f(x)dx, \tag{87}$$

  with matching P_c^1 function $(\Pi^0 f)_h$. It is called the *Clement interpolate* of $f(x)$.

- The piecewise constant orthogonal projection $\bar{\Pi}^0 f(x) \in P^0$ defined on $[x_j, x_{j+1}]$ by

$$\bar{\Pi}^0 f_{j+1/2} = \frac{1}{h} \int_{x_j}^{x_{j+1}} f(x)dx. \tag{88}$$

- The piecewise affine orthogonal projection $\Pi^1 f(x) \in P_c^1$ defined by

$$(f - \Pi^1 f, v_h) = 0 \ , \ \forall v_h \in P_c^1. \tag{89}$$

The following result is easy to verify,

Proposition 4.1 *(i) The HB scheme (42) is equivalent to the mixed finite element method: find $(u_h, p_h) \in P_{c,0}^1 \times P_c^1$ solution of*

$$\begin{cases} -(p_{h,x}, v_h) = (\bar{\Pi}^0 f, v_h) \ , \ \forall v_h \in P_{c,0}^1 \ , \ (a) \\ (p_h - u_{h,x}, q_h) = 0 \ , \ \forall q_h \in P_c^1 \ , \ (b) \end{cases} \tag{90}$$

(ii) $u_h \in P_{c,0}^1$ is the solution of

$$\Big(\Pi^1(u_{h,x}), v_{h,x}\Big) = (\bar{\Pi}^0 f, v_h) \ , \ \forall v_h \in P_{c,0}^1 \tag{91}$$

Note also that $(90)_a$ can be rewritten as

$$-(p_{h,x}, \bar{\Pi}^0(v_h)) = (f, \bar{\Pi}^0(v_h)). \tag{92}$$

The setting of the HB scheme (42) according to the mixed finite element formalism is derived as follows.

Consider

- The bilinear form a defined on $P_c^1 \times P_c^1$ by

$$a(p_h, q_h) = (p_h, q_h). \tag{93}$$

- The bilinear form b defined on $P_c^1 \times P_{c,0}^1$ by

$$b(p_h, v_h) = (p_h, v_{h,x}). \tag{94}$$

Proposition 4.2 *The HB scheme (42) is equivalent to the mixed finite element method:*
find $(u_h, p_h) \in P_{c,0}^1 \times P_c^1$ *solution of*

$$\begin{cases} b(p_h, v_h) = L_f(v_h) \quad , \quad \forall v_h \in P_{c,0}^1 \\ a(p_h, q_h) - b(q_h, u_h) = 0 \ \ , \ \ \forall q_h \in P_c^1, \end{cases} \tag{95}$$

where the linear form L_f *is given by*

$$L_f(v_h) = [(\Pi^0 f)_h, v_h] + \frac{h^2}{6}[(\Pi^0 f_h)_x, v_{h,x}] \quad (= (\bar{\Pi}^0 f, v_h)). \tag{96}$$

The well-posedness and error estimates for (90) are deduced from the following two properties of mixed formulations, see [1, 7, 23, 12]:

- Coercivity of the bilinear form $a(p_h, q_h)$ on the kernel space V_h defined by

$$V_h = \left\{ p_h \in P_c^1 \text{ such that } b(p_h, v_h) = 0 \ \ , \ \ \forall v_h \in P_{c,0}^1 \right\}. \tag{97}$$

  That property is straightforward here since

$$a(p, p) = |p|^2_{L^2[0,1]}. \tag{98}$$

- The inf-sup property of the form $b(p_h, v_h)$ between the spaces P_c^1 and $P_{c,0}^1$, which is

$$\sup_{q_h \in P_c^1, |q_h| \leq 1} |b(q_h, u_h)| \geq C|u_h| \ \ , \ \ \forall u \in P_{c,0}^1. \tag{99}$$

Note that

$$b(q_h, u_h) = (q_h, u_{h,x}) = (\widetilde{\delta}_x u, q)_{h'}. \tag{100}$$

Selecting $q_h \in P_c^1$ matching the grid function $q = \widetilde{\delta}_x u$ gives, for all $u \in l_{h,0}^2$,

$$|b(q_h, u_h)| = |\widetilde{\delta}_x u|^2_{h'} \geq C|u|_h^2 \geq C'|u_h|^2, \tag{101}$$

where we have used (9).

The error estimates deduced from the general theory of mixed form of FEM, [1], [23], [12], allows to obtain the first order error estimate

$$|p - p_h| + |u_x - u_{h,x}| \leq Ch|f|_{L^2[0,1]}. \tag{102}$$

which is less informative than (65).

Observe that the superconvergence properties (65) are more easily detected in the framework of the compact schemes, than in the one of the mixed finite element method.

5 Numerical results

5.1 Introduction

In this section, we display some numerical results which allow to observe practical features of the hermitian box scheme. The scheme that is used is basically (42). In the case of a diffusion function $k(x)$ piecewise continuous, we use a slightly modified version of (42), as explained below. The following observations can be made:

- We observe for regular problems a fourth order accuracy of the scheme for u in both the L^2 and the L^∞ norms.
- We observe for regular problems a remarkable superconvergence result for the gradient, on very coarse grids.
- The scheme is able to produce good approximations, even on under-resolved grids.
- The scheme is able to handle very strong contrasts in the ellipticity coefficient.
- For elliptic problems with high contrasts, the scheme produces in the worst case a first order convergence rate in the discrete H^1 norm, and most of the time a better convergence rate. Furthermore, the levels of the error are much smaller than the usual finite element method.

All the computations have been performed with *matlab*. The discrete L^2, H^1 and L^∞ errors are defined by

$$\begin{cases} |u - u_h|_h = \left[h \sum_i (u(x_i) - u_i)^2 \right]^{1/2} \quad (a), \\ \|u - u_h\|_{1,h} = \left[h \sum_{i=1}^{N} |u_i - u(x_i)|^2 + |p_i - u'(x_i)|^2 \right]^{1/2} \quad (b), \\ |u - u_h|_{\infty,h} = \sup_{j=1,..N} |u(x_i) - u_i| \quad (c). \end{cases} \tag{103}$$

5.2 1D regular Poisson problem

We report here some numerical results for the Poisson problem (19), to verify the accuracy of the solution of scheme (42) for the following exact solutions. Note that the integration of the source term $f(x) = -u''(x)$ is evaluated exactly in $(42)_{a'}$.

- $u(x) = \sin(n\pi x)$, with $n \geq 1$, $0 < x < 1$.
  We observe for different values of n a 4th order convergence rate for u. Furthermore, we observe that the scheme is numerically *exact* for the flux $p(x) = u'(x)$, independently of the parity of N and of the wavenumber n.

- $u(x) = \sin(16\pi x^2), \quad 0 < x < 1$.
  The oscillations are non uniform on $[0, 1]$. To compute the convergence rate, we take a value of h starting from $h = 1/128$, which corresponds to an underresolved grid, to $h = 1/2048$. We observe on Table 1 that the scheme exhibits a superconvergence rate of 2 for u and 4 for p in the L^∞ norm. On Fig. 2, we report the very good behaviour of (u, p)

Mesh size	$\vert u - u_h\vert_h$	$\vert u - u_h\vert_{h,\infty}$	$\vert p - p_h\vert_h$	$\vert p - p_h\vert_{h,\infty}$
nx =129	8.651(-5)	2.899(-3)	4.939(-5)	5.882(-4)
conv. rate	2.87	2.89	4.67	4.16
nx =257	1.180(-5)	3.891(-4)	1.930(-6)	3.273(-5)
conv. rate	2.53	2.42	4.54	4.04
nx =513	2.013(-6)	7.243(-5)	8.274(-8)	1.989(-6)
conv. rate	2.51	2.13	4.51	4.00
nx =1025	3.537(-7)	1.651(-5)	3.628(-9)	1.235(-7)
conv. rate	2.50	2.03	4.50	4.00
nx =2049	6.244(-8)	4.028(-6)	1.600(-10)	7.705(-9)

Table 1: *Error and convergence rate for the 1D Poisson problem with* $u(x) = \sin(16\pi x^2)$.

  on a very coarse 65 points grid with only 5 points per wavelenght near $x = 1$.

5.3 Elliptic 1D problems with high contrasts

We assume here that $k_j = k(x_j)$ are the values of the diffusion $k(x)$ at points x_j. The hermitian box scheme for the elliptic problem (1) is: $U =$

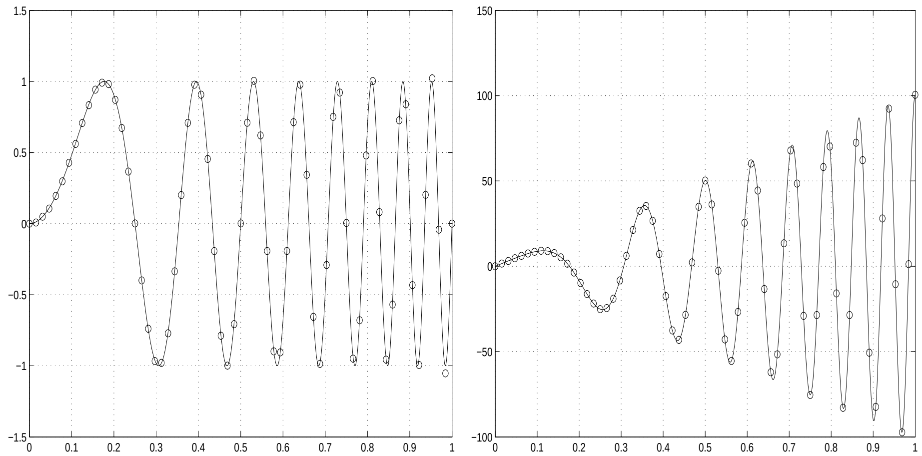

Figure 2: *Solution $u_j \simeq u(x_j)$ and $p_j \simeq u'(x_j)$ of Test Problem (19) with exact solution $u(x) = \sin(16\pi x^2)$, with 65 points ($h = 1/64$), (circles: computed, solid line: exact).*

$[u_1, u_2, ...u_{N-1}, u_N] \in l_0^2$, $P = [p_1, p_2, ...p_{N-1}, p_N] \in l^2$ solution of

$$\begin{cases} -\delta_x(kp)_j = \Pi^0 f_j \ \ , \ \ 2 \leq j \leq N-1 \quad (a) \\ p_j + \dfrac{h^2}{6}\delta_x p_j = \delta_x u_j \ \ , \ \ 2 \leq j \leq N-1 \quad (b) \\ u_1 = u_N = 0, \text{ Dirichlet conditions} \quad (c) \\ p_1 + \dfrac{h}{3}\delta_x^+ p_1 = \delta_x^+ u_1 \quad (d) \\ p_N - \dfrac{h}{3}\delta_x^- p_N = \delta_x^- u_N \quad (e). \end{cases} \tag{104}$$

Note that we still keep the gradient of the solution $p_j \simeq u'(x_j)$ as the secondary unknown, regardless to the fact that this gradient is discontinuous when $k(x)$ is discontinuous. In addition, we do not consider any upscaling of $k(x)$, [22].

Since the Simpson average operator is pertinent only when the exact solution is sufficiently regular, we switch back locally around discontinuity points of $k(x)$ to the following trapezoidal formula for the approximation of the average of the gradient. Specifically, we have used at points x_j in a small neighborhood of a discontinuity point x_0 of $k(x)$ the following scheme

$$\begin{cases} -\delta_x(kp)_j = \Pi^0 f_j \quad (a) \\ p_j + \dfrac{h^2}{4}\delta_x p_j = \delta_x u_j \quad (b). \end{cases} \tag{105}$$

In this section, we report numerical results obtained with the scheme (104-105) on three interesting cases proposed by Nielsen, [24], in his study of the convergence order of the finite element method for elliptic problems with arbitrary small ellipticity. In that case, the convergence results obtained in Section 5 are no longer valid, since in general, the exact solutions belong to the space H^1 and are not more regular.

In all cases, Nielsen reported in [24] first order convergence rates in the full H^1 norm to illustrate the first order convergence rate proved theoretically for elliptic problems with high contrasts, when the source term vanishes in areas of low permeability. In our results, we are specifically interested in practical pointwise superconvergence for u and p, so we provide the error in the discrete H^1 norm $(103)_b$.

- *Case 1* - The problem is

$$\begin{cases} -(k(x)u_x)_x = f(x) \quad , \quad 0 < x < 3 \\ u(0) = 0 \ \ , \ \ u(3) = 1, \end{cases} \tag{106}$$

with a diffusion and source term given by

$$(f(x), k(x)) = \begin{cases} (1,1) & , \ 0 \leq x \leq 1 \\ (0,\delta) & , \ 1 < x < 2 \\ (1,1) & , \ 2 \leq x \leq 3, \end{cases} \tag{107}$$

where $\delta > 0$ is a constant. The numerical results are compared with the exact solution, [24],

$$u(x) = \begin{cases} \frac{3\delta+1}{2\delta+1}x - \frac{1}{2}x^2 \quad , \ 0 \leq x \leq 1, \\ (\frac{3\delta+1}{2\delta+1} - \frac{1}{2}) + \frac{1}{2\delta+1}(x-1) \quad , \ 1 < x < 2, \\ -(\frac{3\delta}{2\delta+1} + \frac{1}{2}) + \frac{5\delta+2}{2\delta+1}x - \frac{1}{2}x^2 \quad , \ 2 \leq x \leq 3. \end{cases} \tag{108}$$

We observe on Table 2 a 1.5 convergence rate in the discrete H^1 norm. On Fig. 3, we display the computed solution on a coarse grid of 61 points with $\delta = 1/16$, in order to observe the good behaviour of the scheme for u and p.

- *Case 2* - The problem is the same as (106) with a diffusion coefficient given in (107), but with a source term replaced in (107) by $f(x) \equiv 1$ for $0 \leq x \leq 3$.

$$u(x) = \begin{cases} \frac{8\delta+3}{4\delta+2}x - \frac{1}{2}x^2 \quad , \ 0 \leq x \leq 1, \\ \frac{3\delta^2-2\delta-1}{\delta(2\delta+1)} + \frac{8\delta+3}{\delta(4\delta+2)}x - \frac{1}{2\delta}x^2 \quad , \ 1 < x < 2, \\ \frac{1-\delta}{2\delta+1} + \frac{8\delta+3}{4\delta+2}x - \frac{1}{2}x^2 \quad , \ 2 \leq x \leq 3. \end{cases} \tag{109}$$

	$\delta = \frac{1}{2}$	$\delta = \frac{1}{4}$	$\delta = \frac{1}{8}$	$\delta = \frac{1}{16}$
h	$\|u - u_h\|_{1,h}$	$\|u - u_h\|_{1,h}$	$\|u - u_h\|_{1,h}$	$\|u - u_h\|_{1,h}$
10^{-1}, nx $= 31$	5.329 (-3)	1.189 (-2)	1.911 (-2)	2.520 (-2)
conv. rate	1.51	1.50	1.51	1.52
20^{-1}, nx $= 61$	1.862 (-3)	4.184 (-3)	6.697 (-3)	8.781 (-3)
conv. rate	1.50	1.50	1.50	1.51
40^{-1}, nx $= 121$	6.557 (-4)	1.476 (-3)	2.358 (-3)	3.083 (-3)
conv. rate	1.50	1.50	1.50	1.50
80^{-1}, nx $= 241$	2.314 (-4)	5.213 (-4)	8.318 (-4)	1.086 (-3)
conv. rate	1.50	1.50	1.50	1.50
160^{-1}, nx $= 481$	8.176 (-5)	1.842 (-4)	2.937 (-4)	3.834 (-4)

Table 2: *Error and convergence rate for Test Case 1 (106, 108).*

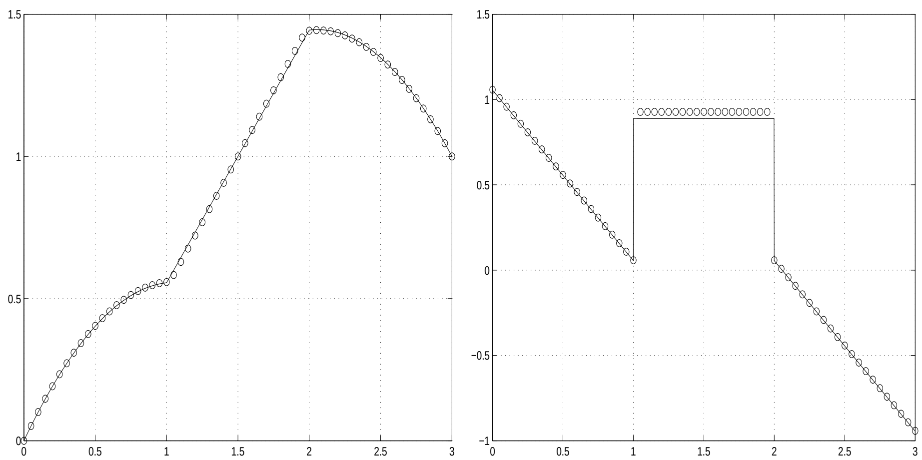

Figure 3: *Solution $u_j \simeq u(x_j)$ and $p_j \simeq u'(x_j)$ of Test Case 1, (106,108) with* 61 *points ($h = 1/20$), $\delta = 1/16$, (circles: computed, solid line: exact).*

We report in Table 3, the results obtained with the scheme (104), (105). The HB scheme is less accurate in that case, with a measured convergence rate of 1 in the discrete H^1 norm, and the convergence rate is not better than the one of the finite element method, with full H^1 norm, [24]. Fig. 4 shows the computed solution in this case on the coarse 61 points grid. Whereas the computed solution appears to be very good on the gradient p, a lack of accuracy is observable on u. An enhancement of the quadrature rule $(105)_b$ seems needed in this case.

- *Case 3* - The third problem in [24] is problem (106) with source term

	$\delta = \frac{1}{2}$	$\delta = \frac{1}{4}$	$\delta = \frac{1}{8}$	$\delta = \frac{1}{16}$
h	$\|u - u_h\|_{1,h}$	$\|u - u_h\|_{1,h}$	$\|u - u_h\|_{1,h}$	$\|u - u_h\|_{1,h}$
10^{-1}, nx $= 31$	2.715(-2)	0.1040	0.2862	0.6770
conv. rate	1.05	1.02	1.01	1.01
20^{-1}, nx $= 61$	1.307(-2)	5.104(-2)	0.1416	0.3360
conv. rate	1.03	1.02	1.00	1.00
40^{-1}, nx $= 121$	6.396(-3)	2.526(-2)	7.042(-2)	0.1674
conv. rate	1.02	1.01	1.00	1.00
80^{-1}, nx $= 241$	3.162 (-3)	1.257 (-2)	3.511 (-2)	8.351 (-2)
conv. rate	1.00	1.00	1.00	1.00
160^{-1}, nx $= 481$	1.572 (-3)	6.267 (-3)	1.753 (-2)	4.171 (-2)

Table 3: *Error and convergence rate for the Test Case 2, (106, 108).*

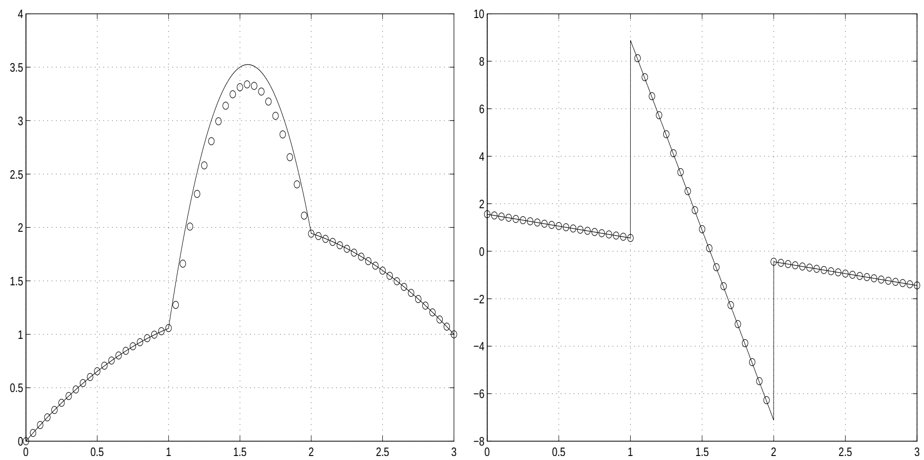

Figure 4: *Solution $u_j \simeq u(x_j)$ and $p_j \simeq u'(x_j)$ of Test Case 2 (106, 109) with* 61 *points ($h = 1/20$), $\delta = 1/16$, (circles: computed, solid line: exact).*

$f(x) \equiv 0$ and the smooth ellipticity coefficient

$$k(x) = \big(x - \frac{3}{2}\big)^2 + \delta \quad , \quad 0 \le x \le 3, \tag{110}$$

with a value δ at abscissa 3/2. The exact solution is

$$u(x) = \big(2 \arctan(\frac{3/2}{\sqrt{\delta}})\big)^{-1} \arctan\big(\frac{x - 3/2}{\sqrt{\delta}}\big) + \frac{1}{2} \quad , \quad 0 \le x \le 3 \tag{111}$$

Since $k(x)$ is a regular function, we use for Case 3 the scheme (42) with the Simpson operator without any modification. We observe on Table 4 a convergence rate of 2.5 in the discrete H^1 norm $(103)_b$, with very good error levels. A superconvergence phenomenon happens also in that case.

	$\delta = \frac{1}{2}$	$\delta = \frac{1}{4}$	$\delta = \frac{1}{8}$	$\delta = \frac{1}{16}$
h	$\|u-u_h\|_{1,h}$	$\|u-u_h\|_{1,h}$	$\|u-u_h\|_{1,h}$	$\|u-u_h\|_{1,h}$
10^{-1}, nx $= 31$	1.4557 (-4)	1.2202 (-4)	1.0681 (-4)	3.1966 (-4)
conv. rate	2.50	2.50	2.61	4.52
20^{-1}, nx $= 61$	2.5721 (-5)	2.1660 (-5)	1.7418 (-5)	1.3947 (-5)
conv. rate	2.50	2.51	2.50	2.50
40^{-1}, nx $= 121$	4.5451 (-6)	3.8112 (-6)	3.0781 (-6)	2.4595 (-6)
conv. rate	2.50	2.50	2.50	2.50
80^{-1}, nx $= 241$	8.0331 (-7)	6.7368 (-7)	5.4412 (-7)	4.3459 (-7)
conv. rate	2.50	2.50	2.50	2.50
160^{-1}, nx $= 481$	1.4200 (-7)	1.1908 (-7)	9.6187 (-8)	7.6822 (-8)

Table 4: *Error and convergence rate for Test Case 3, (106,110).*

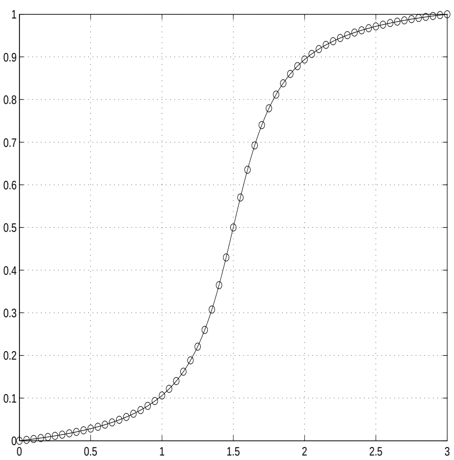

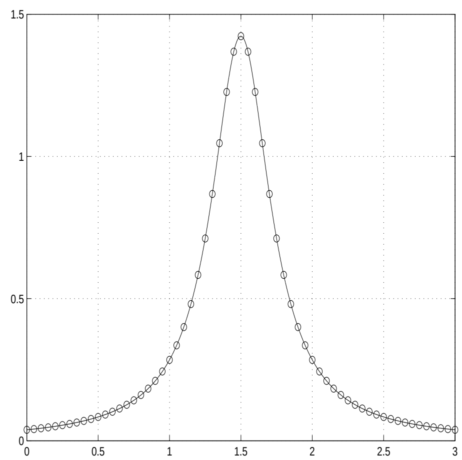

Figure 5: *Solution* $u_j \simeq u(x_j)$ *and* $p_j \simeq u'(x_j)$ *of Test Case 3, (106,110) with* 61 *points* ($h = 1/20$)*, (circles: computed, solid line: exact).*

- *Case 4* - We keep the same problem as in the previous case. In order to demonstrate the behaviour of the HB scheme for problems with an ellipticity coefficient with very high contrasts and smooth variations, we give in Table 5 the levels of the errors in the discrete H^1 norm for a value of the parameter $\delta = 1/64, 1/256, 1/2048, 1/8192$ on grids with h from $3/40$ to $h = 3/2560$. The convergence rate seems to tend to 2.5 after a superconvergence phase. The levels of the errors on the final grid are very good.

	$\delta = \frac{1}{64}$	$\delta = \frac{1}{256}$	$\delta = \frac{1}{2048}$	$\delta = \frac{1}{8192}$
h	$\|u - u_h\|_{1,h}$	$\|u - u_h\|_{1,h}$	$\|u - u_h\|_{1,h}$	$\|u - u_h\|_{1,h}$
3/40, nx = 41	3.648 (-3)	6.737 (-2)	0.354	1.073
conv. rate	8.33	4.28	2.43	1.61
3/80, nx = 81	1.135 (-5)	3.469 (-3)	6.562 (-2)	0.351
conv. rate	3.83	8.08	4.30	2.44
3/160, nx = 161	7.984 (-7)	1.285 (-5)	3.338 (-3)	6.477 (-2)
conv. rate	2.54	6.59	8.03	4.28
3/320, nx = 321	1.368 (-7)	1.332 (-7)	1.272 (-5)	3.333 (-3)
conv. rate	2.50	3.00	8.01	8.05
3/640, nx = 641	2.414 (-8)	1.660 (-8)	4.921 (-8)	1.255 (-5)
conv. rate	2.50	2.54	4.12	5.72
3/1280, nx = 1281	4.266 (-9)	2.845 (-9)	2.830 (-9)	2.387 (-8)
conv. rate	2.50	2.50	2.99	4.50
3/2560, nx = 2561	7.541 (-10)	5.019 (-10)	3.545 (-10)	1.050 (-9)

Table 5: *Error and convergence rate for Test Case 4, (106), (110)*

6 Conclusion

We have presented a finite difference scheme apparently new in its design, combining the computation of the gradient of the solution using a hermitian collocation method, with a discrete version of the conservation law at the level of a box of lenght $2h$. This scheme allows to have a local accuracy for u and p directly linked to the one of a quadrature rule, and good stability properties. The numerical results displayed on elliptic problems with high contrasts in the diffusion coefficient seem very promising. The levels of error are especially good on the gradient p. Further investigations on the design of the quadrature rule for the gradient are clearly needed, to have a better understanding of the stability and convergence properties of the scheme. Furthermore, the extension to multidimension is in progress.

Acknowledgement: The author expresses his gratitude to an anonymous referee for his constructive critics which helped greatly to enhance this paper.

References

[1] I. Babuška. Error-bounds for finite elements method. *Numer. Math*, 16:322–333, 1973.

[2] J.T. Beals and A. T. Layton. On the accuracy of finite difference methods for elliptic problems with interfaces. Preprint 2005, Duke Univer-

sity.

[3] M. Ben-Artzi, J-P. Croisille, and D. Fishelov. Convergence of a compact scheme for the pure streamfunction formulation of the unsteady Navier-Stokes system. *SIAM J. Numer. Anal.*, 2006 *to appear*.

[4] M. Ben-Artzi, J-P. Croisille, D. Fishelov, and S. Trachtenberg. A Pure-Compact Scheme for the Streamfunction Formulation of Navier-Stokes equations. *Jour. Comp. Phys.*, 205(2):640–664, 2005.

[5] C. Bernardi, C. Canuto, and Y. Maday. Generalized inf-sup conditions for Chebyshev spectral approximation of the Stokes problem. *SIAM J. Numer. Anal*, 25,6:1237–1271, 1988.

[6] B. Bialecki, G. Fairweather, and K.R. Bennett. Fast direct solvers for piecewise Hermite bicubic orthogonal spline collocation equations. *SIAM J. Numer. Anal.*, 29:156–173, 1992.

[7] F. Brezzi. On the existence, uniqueness and approximation of saddle-point problems, arising form lagrangian multipliers. *R.A.I.R.O.*, 8:129–151, 1974.

[8] S.H. Chou, D.Y. Kwak, and O. Vassilevski. Mixed covolume methods for elliptic problems on triangular grids. *SIAM J. Numer. Anal.*, 35(5):1850–1861, 1998.

[9] L. Collatz. *The Numerical Treatment of Differential Equations*. Springer-Verlag, 3-rd edition, 1960.

[10] B. Courbet. Two-point schemes for computational fluid dynamics. *La Recherche Aérospatiale*, 5:21–46, 1990.

[11] B. Courbet and J-P. Croisille. Finite volume box schemes on triangular meshes. *Math. Model. and Numer. Anal.*, 32(5):631–649, 1998.

[12] J-P. Croisille. Finite volume box-schemes and mixed methods. *Math. Model. and Numer. Anal.*, 34(5):1087–1106, 2000.

[13] J-P. Croisille. Keller's box-scheme for the one-dimensional stationary convection-diffusion equation. *Computing*, 68:37–63, 2002.

[14] J-P. Croisille and I. Greff. Some box schemes for elliptic problems. *Numer. Methods Partial Differential Equations*, 18(3):355–373, 2002.

[15] E. Elsaesser and R. Peyret. Méthodes hermitiennes pour la résolution des équations de Navier-Stokes. Technical Report TP 1978-138, ONERA, 1978.

[16] I. Greff. *Schémas boîte: Etude théorique et numérique.* PhD thesis, Université de Metz, France, 2003.

[17] W. Hackbusch. On first and second order box schemes. *Computing*, 41:277–296, 1989.

[18] G. Hämmerlin and K-H. Hoffmann. *Numerical Mathematics.* Springer-Verlag, 1991.

[19] B. Heinrich. *Finite Difference methods on Irregular Networks*, volume 82 of *Int. Series Num. Math.* Birkhauser, 3-rd edition, 1987.

[20] H. B. Keller. A new difference scheme for parabolic problems. In *Numerical Solution of Partial Differential Equations, II (SYNSPADE 1970) (Proc. Sympos., Univ. of Maryland, College Park, Md., 1970)*, pages 327–350. Academic Press, New York, 1971.

[21] S. K. Lele. Compact finite-difference schemes with spectral-like resolution. *J. Comput. Phys.*, 103:16–42, 1992.

[22] R. Luce and S. Perez. A numerical upscaling method for an elliptic equation with heterogeneous tensorial coefficients. *Int. Journal for Numerical Methods in Engineering*, 54:537–556, 2002.

[23] R.A. Nicolaides. Existence, uniqueness and approximation for generalized saddle point problems. *SIAM J. Numer. Anal*, 19,2:349–357, 1982.

[24] B.F. Nielsen. Finite element discretizations of elliptic problems in the presence of arbitrarily small ellipticity; an error analysis. *SIAM J. Numer. Anal.*, 36(2):368–392, 1998.

[25] M.J.D. Powell. *Approximation theory and methods.* Cambridge University Press, 1981.

[26] M. H. Protter and H. F. Weinberger. *Maximum Principles in Differential Equations.* Springer, 1984.

[27] P-A. Raviart and J-M. Thomas. A mixed finite element method for 2nd order elliptic problems. In *Mathematical Aspects of Finite Element Methods. Lecture Notes in Math.*, volume 606, pages 292–315. Springer, Berlin, 1977.

[28] J. W. Stephenson. Single cell discretizations of order two and four for biharmonic problems. *J.Comp.Phys.*, 55:65–80, 1984.

[29] D. Yang. Finite elements for elliptic problems with wild coefficients. *Mathematics and Computers in Simulation*, 54:383–395, 2000.

Jean-Pierre Croisille
Laboratoire Mathématiques et Applications de Metz, UMR 7122
Université de Metz, F-57045 Metz Cedex
Ile du Saulcy
Metz
France
jean-pierre.croisille@univ-metz.fr